Electrochemistry Communications 72 (2016) 118–121

Contents lists available at ScienceDirect

Electrochemistry Communications

journal homepage: www.elsevier.com/locate/elecom

Efficient charge separation promoting visible-light-driven photocatalytic activity of MnO_x decorated WS_2 hybrid nanosheets

Hua-Bin Fang, Nan Li, Zhibing Xue, Yikun Zhang, Yan-Zhen Zheng *, Xia Tao *

State Key Laboratory of Organic-Inorganic Composites, Beijing University of Chemical Technology, Beijing 100029, China

ARTICLE INFO

Article history:
Received 26 July 2016
Received in revised form 7 September 2016
Accepted 19 September 2016
Available online 20 September 2016

Keywords:
Tungsten disulfide
Manganese oxide
Charge separation
Hole-trapping
Visible-light-driven photocatalyst

ABSTRACT

Tungsten disulfide (WS_2) has recently emerged as a narrow-band visible-light-driven photocatalyst; however, high recombination of photo-induced electrons and holes becomes a major concern to advance its photocatalytic performance. Here we for the first time adopt manganese oxide (MnO_x) as a hole-trapping material to decorate WS_2 nanosheets by photo-deposition in $MnSO_4$ solution. The MnO_x decorated WS_2 (MnO_x/WS_2) is found to exhibit more negative flat band potential, lower impedance and higher photocurrent response compared with pure WS_2. These features beneficial to charge transfer and separation render the MnO_x/WS_2 nanosheets highly active and visible-light-driven photocatalyst in RhB degradation. Further, the hole-trapping function of MnO_x in promoting efficient charge separation of MnO_x/WS_2 is experimentally demonstrated.

1. Introduction

Since the first report on photocatalytic (PC) water splitting by TiO_2 under ultraviolet light [1,2], solar photocatalysis for remediation of environmental pollutants and hydrogen production from water has attracted a tremendous amount of interest as it offers direct use of sunlight for energy and environmental applications [3–8]. As one of typical materials in transition metal dichalcogenides allotrope, tungsten disulfide (WS_2) shows a unique combination of valuable structural, electronic, optical, mechanical, chemical, and thermal properties that have been studied for decades [9–15]. The bandgap of WS_2 is ~1.35 eV, which expands the light absorption region to ~910 nm, completely covering the visible region of solar spectrum [10,16]. Furthermore, the valence and conduction band edges of WS_2 are suitable to drive the necessary redox chemistry for photocatalysis [7,10,12,16,17]. However, the narrow bandgap of WS_2 will inevitably cause high recombination of photo-induced electrons and holes, retarding its PC activity. Therefore, efficient charge separation for advancing the PC activity of WS_2 becomes a key issue.

Recent investigations on manganese oxide (MnO_x) anchored to Bi-based photocatalysts (such as $BiVO_4$ and BiOI) have shown that MnO_x as active/reaction sites can provide trapping sites for the photogenerated holes to inhibit carrier recombination [18–20]. As such, utilizing the decoration with MnO_x could be a suitable approach to promote the separation efficiency of photo-induced charge carriers of WS_2, which has yet to be reported until now.

In this communication, we for the first time use MnO_x as a hole-trapping material to promote the charge separation efficiency of WS_2. MnO_x decorated WS_2 (MnO_x/WS_2) hybrid nanosheets were prepared by photo-deposition in $MnSO_4$ solution, and characterized by scanning electron microscope (SEM), energy-dispersive spectroscopy (EDS), X-ray photoelectron spectroscopy (XPS), Mott-Schottky (M-S) analysis, electrochemical impedance spectroscopy (EIS) and amperometric i-t curve. We find that MnO_x/WS_2 exhibits more negative flat band potential (E_{fb}), lower impedance, and higher photocurrent response compared with pristine WS_2. Herein, rhodamine B (RhB), a nonbiodegradable xanthane dye in the aqueous ecosystem, was chosen as a representative probe to evaluate the photocatalytic activity of the as-obtained MnO_x/WS_2 nanosheets. As a result, the visible-light-driven PC activity of MnO_x/WS_2 is significantly enhanced. Furthermore, the hole-trapping function of MnO_x in promoting efficient charge separation of WS_2, which consequently boosts the PC activity, has also been demonstrated.

2. Experimental

The MnO_x/WS_2 hybrid nanosheets were prepared by photo-deposition. Typically, 1 g WS_2 (Aladdin, 99.9%) and 50 mg $MnSO_4$ (Tianjin Fuchen, AR) were mixed in 100 mL deionized water. The suspension was then irradiated by a 300 W Xe lamp (CEL-HXF300) under continuous stirring. After 5 h of photo-deposition, the suspension was centrifuged and rinsed, followed by drying at 60 °C overnight. The black MnO_x/WS_2 powder was obtained. For the MnO_x/WS_2 film, a slurry

* Corresponding authors.
E-mail addresses: zhengyz@mail.buct.edu.cn (Y.-Z. Zheng), taoxia@mail.buct.edu.cn (X. Tao).

http://dx.doi.org/10.1016/j.elecom.2016.09.020
1388-2481/

containing 1 g WS_2 and 1.5 mL terpineol in an ethanol solution was prepared via rotary evaporation and subsequently coated on a fluorine-doped tin oxide (FTO) glass substrate via a typical doctor blading method. The decoration of MnO_x on the WS_2 film follows the photo-deposition procedure similar to MnO_x/WS_2 powder.

Electrochemical and photoelectrochemical measurements were carried out on an electrochemical workstation (CHI660C, ShangHai) in a three-electrode system, using 0.5 M Na_2SO_4 solution as the electrolyte. A 300 W Xe lamp with a 420 nm cut-off was used to guarantee irradiation only by visible light. The light intensity at the electrode surface is determined as ~250 mW/cm^2. The PC activity was evaluated by decomposition of RhB aqueous solution (initial concentration of RhB = 1×10^{-5} mol/L, photocatalyst amount = 50 mg, and total volume = 50 mL) under visible light irradiation. Analytical grade RhB was purchased from Tianjin Fu Chen Chemicals Co. Photoelectrocatalysis was carried out in the three-electrode system using a 2.5 × 3 cm^2 photocatalyst film at a bias potential of −0.5 V vs SCE. Triethanolamine (TEOA, 1 mL) as trapping reagent was used to detect the generation of active holes in the PEC process.

3. Results and discussion

The photo-deposition of MnO_x on the surface of WS_2 was carried out using $MnSO_4$ as a precursor and water as an electron scavenger. Under photo-irradiation the photogenerated holes on WS_2 are readily available for the photo-oxidation of Mn^{2+} into MnO_x accompanying the elimination of photogenerated electrons by water scavenger. Similar mechanisms have also been reported in MnO_x modified $BiVO_4$ or BiOI [18–20]. The SEM images in Fig. 1a&b show the morphological features of WS_2 and MnO_x/WS_2. WS_2 displays a hexagonal nanosheet structure in shape (Fig. 1a). For MnO_x/WS_2, the hexagonal nanosheet structural feature remains constant except for MnO_x nanoparticles dispersed on the surface of WS_2 nanosheets (Fig. 1b). The EDS spectrum of MnO_x/WS_2 exhibits the peaks related to elemental W, S, O and Mn (Fig. 1c). The atomic content of Mn in the hybrid MnOx/WS_2 sample is measured as ~1 at.%. The surface chemical composition and chemical valence state of the elements in MnO_x/WS_2 are checked by XPS (Fig. 1d–f). Peaks located at 33.1, 35.3, and 38.7 eV are ascribed to W $4f_{7/2}$, W $4f_{5/2}$, and W $5p_{5/2}$, respectively (Fig. 1d). The peaks of S $2p_{3/2}$ and S $2p_{1/2}$ orbital of divalent sulfide ions are observed at 162.9 and 164.0 eV, respectively (Fig. 1e). The bonding energy of the elements is consistent with the W^{4+} and S^{2-} in WS_2 [16]. The two peaks of the Mn 2p region at 641.8 and 654.2 eV are assigned to Mn $2p_{3/2}$ and Mn $2p_{1/2}$, respectively, as shown in Fig. 1f. Based on their binding energies, it can be reasonably concluded that MnO_x forms on the surface of WS_2 [18,20].

Fig. 2a shows the M-S plots of WS_2 and MnO_x/WS_2. According to the M-S equation:

$$1/C_{sc}{}^2 = 2(E - E_{fb} - \kappa T/e)/(e\varepsilon\varepsilon_0 N_D)$$

where C_{sc} is the total capacitance of the space charge region, E is potential, E_{fb} is the flat band potential, κ is Boltzmann's constant, T is temperature, ε is permittivity in vacuum, ε_0 is dielectric constant, N_D is charge carrier density. The negative slopes of the two lines show that both WS_2 and MnO_x/WS_2 are n-type semiconductor [21,22]. N_D was calculated according to the linear slope of the M-S plot, and it turns out to be larger for MnO_x/WS_2 film (5.6×10^{19} cm^{-3}) in comparison with pure WS_2 film (3.6×10^{19} cm^{-3}). The results indicate that the presence of MnO_2 leads to an increase in the number of charge carriers, which have a positive effect in lowering the charge transfer resistance. The E_{fb} of WS_2 and MnO_x/WS_2 calculated according to the intercept with the potential axis are −0.68 V (vs SCE) and −0.78 V (vs SCE), respectively. It is found that after MnO_x-decorating, the value of E_{fb} shifts negatively. As for the n-type WS_2 semiconductor, negative shift of E_{fb} causes the increase of upward band bending i.e. the enhancement of the near-surface electric field in the bent-band region, and finally facilitating the effective separation of electron-hole pairs [23]. Apparently, MnO_x-decorating enhances the charge transfer and separation ability of MnO_x/WS_2.

It is well established that EIS Nyquist plots are associated with charge transfer resistance [21,24]. The radius of the arc in the EIS spectra reflects the interface layer resistance occurring at the electrode surface, and a smaller arc radius implies a lower charge transfer resistance [25]. A remarkable decrease in Nyquist plots arc radius for MnO_x/WS_2 is observed (Fig. 2b), which suggests that charge transfer resistance of MnO_x/WS_2 is much smaller than that of pure WS_2. Note that the reduction of charge transfer resistance is believed to be beneficial to efficient charge separation [26,27].

Moreover, transient photocurrent responses of the MnO_x/WS_2 photocatalyst can directly correlate with the separation efficiency of the photogenerated carriers [20,26,28]. Fig. 2c presents the results of transient photocurrent responses obtained from the MnO_x/WS_2 and pure WS_2 films. The photocurrent generates when the light is on and decreases to zero when the light is turned off. It is clear that the photocurrent of MnO_x/WS_2 is obviously larger than that of pure WS_2. The enhanced photocurrent activity of MnO_x/WS_2 indicates more efficient separation of photo-induced electron-hole pairs in MnO_x/WS_2 than in

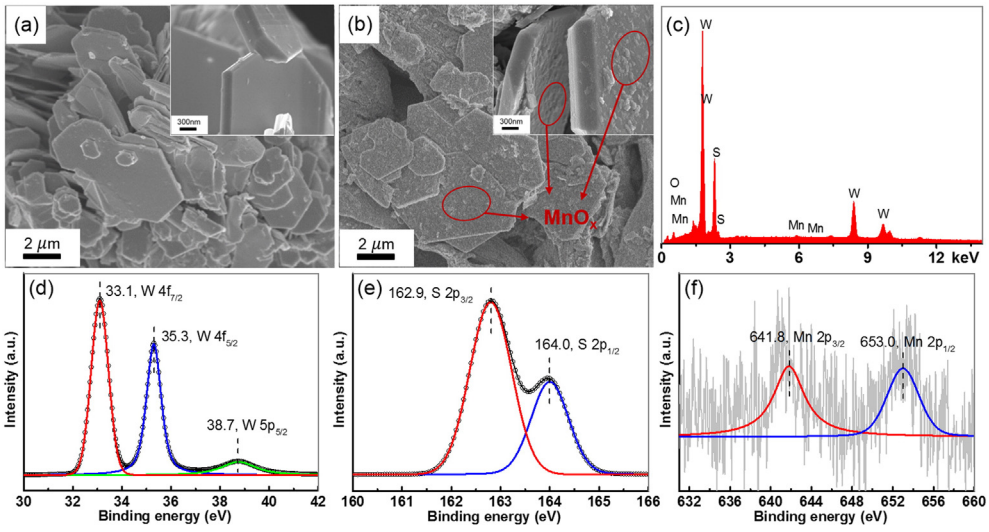

Fig. 1. (a, b) SEM images of WS_2 (a) and MnO_x/WS_2 (b), inset of (a) and (b) are the magnified SEM images of WS_2 and MnO_x/WS_2 respectively. (c) EDS spectrum of MnO_x/WS_2. (d–f) XPS scan of W 5p and W 4f (d), S 2p (e), and Mn 2p (f) for MnO_x/WS_2.